

Anisotropic Compact Stellar Objects in Modified Gauss-Bonnet Gravity

M. Sharif ^{*} and Amna Ramzan [†]

Department of Mathematics, University of the Punjab,
Quaid-e-Azam Campus, Lahore-54590, Pakistan.

Abstract

This paper is devoted to studying anisotropic compact stellar structures by adopting embedding class-1 technique in the background of modified Gauss-Bonnet gravity. The unknown constants are evaluated by the matching of interior spacetime with the Schwarzschild exterior geometry corresponding to $f(\mathcal{G}) = \chi \mathcal{G}^n$ model, where χ and n are positive constants. The observed masses of compact star candidates (SAX J1808.4-3658, Vela X-1, PSR J0348+0432, 4U 1608-52) are used with the condition of vanishing radial pressure at the stellar surface to predict their radii. We have examined viability and stability of the resulting solution through graphical behavior of matter variables, energy constraints, adiabatic index and causality condition. It is found that embedding class-1 solution for anisotropic compact stars is viable and stable in this theory.

Keywords: $f(\mathcal{G})$ theory; Compact stars; Anisotropy.

PACS: 04.40.Dg; 04.50.Kd; 97.60.Jd.

1 Introduction

In the present age, the cosmological and astrophysical scenarios have motivated many researchers to discuss the universe and its mysterious constituents. Stars are considered as the fundamental component of galaxy as

^{*}msharif.math@pu.edu.pk

[†]amnaramzan2168@gmail.com

well as the main ingredient of astrophysics. The fusion reactions play vital role in the structure formation and evolution of astronomical objects. The fusion process generates the outward directed pressure inside a star which is balanced by the inward directed force of gravity to keep the star in equilibrium state. Once the nuclear fuel is burnt out completely, there appears no enough pressure to stop the star collapse. This leads to the formation of new compact objects categorized as white dwarfs, neutron stars and black holes.

The interior geometry of compact stars provokes the researchers to study the surprising characteristics of celestial objects. The presence of anisotropy in spherically symmetric objects influences important physical characteristics of relativistic objects. Ruderman [1] proposed that nuclear matter possesses anisotropy if the matter density for relativistic object is equal to $10^{15}g/cm^3$. The pressure anisotropy in matter distribution occurs due to viscosity, phase transition [2], pion condensation [3] and super fluid [4]. Many people studied the effects of anisotropy on mass, radius and redshift of the stars by considering the radial and tangential components of pressure. Herrera and Santos [5] analyzed the causes and effects of anisotropy for self-gravitating system. Harko and Mak [6] studied the interior solutions for anisotropic celestial objects and observed their physical features. Dev and Gleiser [7] examined the stability of anisotropic stellar objects in Newtonian and general relativistic unit. Hossein et al. [8] analyzed the stability of anisotropic objects along with the effects of cosmological constant by adopting Krori-Barua solution. Paul and Deb [9] found feasible solutions for compact objects under the influence of pressure anisotropy.

Different techniques, such as constraints on the matter constituents or a particular form of equation of state, are used to formulate the interior solutions of stellar models. The embedding of curved geometry into higher-dimensional spacetime also provides a relation between two potentials (temporal and radial) which helps in finding a solution of the field equations. The technique in which n -dimensional manifold \mathcal{M}_n is embedded into $(n+k)$ -dimensional manifold \mathcal{M}_k is named as embedding class- k for \mathcal{M}_n , where k is the minimum number of extra dimension. Eisenhart [10] defined the embedding class-1 condition to find solutions for static spherically symmetric geometry. Maurya et al. [11] found a new star model of embedding class-1 with different potential functions. The same authors [12] discussed the stability and physical characteristics of anisotropic compact objects by using embedding class-1 technique. Singh and Pant [13] used the same approach to find solutions that describe the internal geometry of astrophysical objects.

Bhar et al. [14] found anisotropic solutions through this technique and examined the behavior of different compact stellar models. Singh et al. [15] analyzed a new model of compact stars (free from geometric singularity) by the embedding of 4-dimensional space into 5-dimensional pseudo-Euclidean geometry.

The mysteries behind the current accelerated expansion of cosmos has attracted the attention of modified gravitational theories. These theories have widely been employed to provide the information about hidden aspects of dark energy and dark matter. The $f(\mathcal{R})$ theory is considered as the simplest extension to general relativity, obtained by using generic function $f(\mathcal{R})$ of Ricci scalar (\mathcal{R}) in the Einstein-Hilbert action. Capozziello et al. [16] investigated the hydrostatic equilibrium of stellar structures in the framework of $f(\mathcal{R})$ gravity. Nojiri and Odintsov [17] inspected the compatibility of modified theories with local tests. Olmo [18] applied Palatini approach in the context of $f(\mathcal{R})$ and $f(\mathcal{R}, \mathcal{Q})$ theories to analyze the aspects related to dark energy, dark matter and quantum gravity. Zubair and Abbas [19] discussed the mathematical modeling of compact stars with static anisotropic interiors by considering the Krori-Barua spacetime in (\mathcal{R}, T) gravity. Yousaf et al. [20] explored the role of different forces as well as equation of state parameter on a viable configuration of anisotropic spherical structures in the same theory.

Nojiri and Odintsov [21] introduced another modified theory referred to as $f(\mathcal{G})$ gravity, where \mathcal{G} represents Gauss-Bonnet invariant term given by $\mathcal{G} = \mathcal{R}^2 - 4R_{\alpha\beta}\mathcal{R}^{\alpha\beta} + \mathcal{R}_{\alpha\beta\xi\eta}\mathcal{R}^{\alpha\beta\xi\eta}$. They discussed different cosmological aspects that describe the accelerated expansion of the universe and possible phase transition from deceleration to acceleration in $f(\mathcal{R})$, $f(\mathcal{G})$ and $f(\mathcal{R}, \mathcal{G})$ theories [22]. Bamba et al. [23] analyzed the finite future time singularities in $f(\mathcal{R}, \mathcal{G})$ as well as $f(\mathcal{G})$ theory and studied possible solutions by involving higher-order curvature terms. Nojiri and Odintsov [24] also studied various relations between modified theories and concluded that such theories may provide the description of inflation with dark energy epoch. Oikonomou [25] discussed bounce cosmology with a Type IV singularity at the bouncing point in the framework of $f(\mathcal{G})$ gravity. He examined that mimetic vacuum $f(\mathcal{G})$ gravity can explain the singular bounce cosmology. Nojiri et al. [26] discussed some issues and the developments of modified gravity such as late time acceleration, inflation and bouncing cosmology. They demonstrated that $f(\mathcal{R})$, $f(\mathcal{G})$ and $f(T)$ theories provide the required description of the universe.

Felice and Tanaka [27] analyzed the behavior of perturbations in the background of $f(\mathcal{R}, \mathcal{G})$ gravity and showed that the existence of ghost is inevitable for generic models. Moreover, they discussed some special cases which avoid the existence of ghost. Nojiri et al. [28] proposed a technique for Gauss-Bonnet theories ($f(\mathcal{G})$ and $f(\mathcal{R}, \mathcal{G})$) to eliminate the ghost modes in the equations of motion. The variation of action integral with respect to perturbed metric tensor yields the perturbed field equations. It is shown that these equations contain fourth order derivatives of the metric with respect to time coordinate. Therefore, ghost modes might appear in $f(\mathcal{G})$ model. They applied constraints on the action integral and used the technique of Lagrange multiplier to produce ghost-free modes. Nojiri et al. [29] studied the inflationary aspects of ghost-free $f(\mathcal{G})$ gravity. By using the method of slow-roll approximation, they calculated the slow-roll and observational indices. The results were consistent with the latest Planck data [28]. Furthermore, they discussed cosmological evolution in the presence of exponentially evolving Hubble rate by considering a coupling function. They demonstrated that the ghost-free model can produce inflationary phenomenon which is compatible with the observational data [29].

Abbas et al. [31] inspected the anisotropic behavior of compact stars using Krori-Barua spacetime in $f(\mathcal{G})$ gravity and analyzed physical characteristics for different star models. Sharif and Fatima [32] investigated the isotropic and anisotropic spherical symmetric solutions in this theory by assuming linear equation of state (EoS). Sharif and Naz [33] examined the gravitational collapse in the same scenario with electromagnetic effects and concluded that there is a decrease in collapsing rate due to modified terms. Sharif and Saba [34] studied the anisotropic solutions of compact stellar objects with Karmarkar constraint in the same theory. The same authors [35] also discussed the effects of charge on gravitational decoupled sources and checked the stability as well as viability of the obtained solutions.

Odintsov [36] proposed a new technique to discuss the equations of motion, slow-roll and the corresponding observational indices in Einstein-Gauss-Bonnet theories of gravity. Oikonomou and Fronimos [37] discussed the non-minimal kinetic coupling corrected Einstein-Gauss-Bonnet theories by considering the GW17017 event with the assumption that the gravitational wave propagates at the speed of light. They also showed that GW170817 is compatible with the recent Planck data [30]. Astashenok [38] studied the data compiled by the LIGO collaboration [39] for the GW190814 event and showed that this event can be represented through some models in the

background of extended theories of gravity. They consider some particular $f(\mathcal{R})$ models to study rotating stars and found that the obtained results were consistent with the findings LIGO. Recently, Shamir and Naz [40] inspected some compact stellar objects corresponding to Tolman-Kuchowicz spacetime in the background of $f(\mathcal{G})$ theory. They consider the observed data of Cen X -3, EXO 1785-248 and LMC X - 4 star models.

In this paper, we explore anisotropic spherical solution by using embedding class-1 technique for a specific $f(\mathcal{G})$ model. We discuss features like evolution of matter variables, mass-radius relation, the Tolman-Oppenheimer-Volkoff (TOV) equation, energy bounds, compactness factor, redshift parameter and stability. The paper has the following format. Section 2 formulates the field equations and solutions using embedding class-1 condition. In section 3, we evaluate unknown constants by smooth matching of interior and exterior geometries at the boundary. Section 4 explores physical features of the obtained solution for some specific compact star models. In the last section, we summarize our results.

2 Field Equations for Anisotropic Source

The action for $f(\mathcal{G})$ theory is defined as [21]

$$\mathcal{A}_{f(\mathcal{G})} = \int \left(\frac{\mathcal{R} + f(\mathcal{G})}{2\kappa^2} + \mathcal{L}_m \right) \sqrt{-g} d^4x, \quad (1)$$

where $f(\mathcal{G})$ is the arbitrary function of Gauss-Bonnet invariant, g represents determinant of the metric tensor ($g_{\alpha\beta}$) and \mathcal{L}_m is the Lagrangian density of matter. Variation of this action with respect to $g_{\alpha\beta}$ leads to

$$\begin{aligned} G_{\alpha\beta} &= \kappa^2 T_{\alpha\beta} + \frac{1}{2} g_{\alpha\beta} f(\mathcal{G}) - (2\mathcal{R}\mathcal{R}_{\alpha\beta} - 4\mathcal{R}_{\alpha}^{\xi}\mathcal{R}_{\xi\beta} - 4\mathcal{R}_{\alpha\xi\beta\eta}\mathcal{R}^{\xi\eta} + 2\mathcal{R}_{\alpha}^{\xi\eta\delta} \\ &\times \mathcal{R}_{\beta\xi\eta\delta}) f_{\mathcal{G}}(\mathcal{G}) - (2\mathcal{R}g_{\alpha\beta}\nabla^2 - 2\mathcal{R}\nabla_{\alpha}\nabla_{\beta} - 4g_{\alpha\beta}\mathcal{R}^{\xi\eta}\nabla_{\xi}\nabla_{\eta} - 4\mathcal{R}_{\alpha\beta}\nabla^2 \\ &+ 4\mathcal{R}_{\alpha}^{\xi}\nabla_{\beta}\nabla_{\xi} + 4\mathcal{R}_{\beta}^{\xi}\nabla_{\alpha}\nabla_{\xi} + 4\mathcal{R}_{\alpha\xi\beta\eta}\nabla^{\xi}\nabla^{\eta}) f_{\mathcal{G}}(\mathcal{G}), \end{aligned} \quad (2)$$

where $f_{\mathcal{G}}(\mathcal{G})$ is the derivative with respect to \mathcal{G} , $\nabla^2 = g^{\alpha\beta}\nabla_{\alpha}\nabla_{\beta}$ and ∇_{α} denotes the covariant derivative. The stress-energy tensor is expressed by

$$T_{\alpha\beta} = g_{\alpha\beta}\mathcal{L}_m - 2\frac{\partial\mathcal{L}_m}{\partial g^{\alpha\beta}}. \quad (3)$$

We take anisotropic matter distribution of stellar objects described by

$$T_{\alpha\beta} = (\rho + p_t)\mathcal{V}_\alpha\mathcal{V}_\beta - p_t g_{\alpha\beta} + (p_r - p_t)\mathcal{U}_\alpha\mathcal{U}_\beta, \quad (4)$$

where ρ , p_t and p_r represent the energy density, tangential and radial pressures, respectively. Also, \mathcal{V}_α indicates the four-velocity and \mathcal{U}_α represents the four-vector in radial direction in comoving frame that satisfy

$$\mathcal{V}^\alpha\mathcal{V}_\alpha = 1, \quad \mathcal{U}_\alpha\mathcal{U}^\alpha = -1.$$

The most interesting feature of $f(\mathcal{G})$ theory is that it may neglect the ghost terms and regularize the action due to Gauss-Bonnet invariant. In order to study the structural properties of compact objects, we take a power-law model of $f(\mathcal{G})$ theory [41]

$$f(\mathcal{G}) = \chi\mathcal{G}^n, \quad (5)$$

where χ denotes the arbitrary constant and $n > 0$ with $n \neq 1$. Here, we choose $\chi = 1$ and $n = 2$. The action (1) with the considered form of $f(\mathcal{G})$ is compatible with the observational data of the expanding universe [42]. The generic function $f(\mathcal{G})$ is viable, since it is compliant with solar system constraints [41]. Moreover, any $f(\mathcal{G})$ model is said to be viable if the generic function and its derivatives are regular. These conditions are fulfilled by the considered model. To discuss the internal geometry of compact stars, we consider static and spherically symmetric metric

$$ds^2 = e^{\nu(r)}dt^2 - e^{\lambda(r)}dr^2 - r^2(d\theta^2 + \sin^2\theta d\phi^2), \quad (6)$$

where $\lambda(r)$ and $\nu(r)$ represent the gravitational metric potentials which depend on radial coordinate r only. Equations (2) and (4)-(6) yield the following field equations

$$\begin{aligned} e^{-\lambda}\left(\frac{\lambda'}{r} - \frac{1}{r^2}\right) + \frac{1}{r^2} &= \frac{\mathcal{G}^2}{2} + 8\pi\rho + \left[\frac{e^{-2\lambda}}{r^2}\left(2(e^\lambda - 3)\right.\right. \\ &\times (2\mathcal{G}'\lambda' - \mathcal{G}\lambda'\nu') + 2(e^\lambda - 1)(2 \\ &\times \mathcal{G}\nu'' + \mathcal{G}(\nu')^2 - 4\mathcal{G}''))\Big], \quad (7) \\ e^{-\lambda}\left(\frac{1}{r^2} + \frac{\nu'}{r}\right) - \frac{1}{r^2} &= -\frac{\mathcal{G}^2}{2} + 8\pi p_r + \left[\frac{e^{-2\lambda}}{r^2}\left(2(e^\lambda\right.\right. \\ &- 3)(\mathcal{G}\lambda'\nu' + 2\mathcal{G}'\nu') - 2(e^\lambda - 1) \end{aligned}$$

$$\begin{aligned}
& \times (2\mathcal{G}\nu'' + \mathcal{G}(\nu')^2)) \Big], \quad (8) \\
\frac{e^{-\lambda}}{2} \left(-\frac{\lambda'\nu'}{2} + \nu'' + \frac{\nu'^2}{2} + \frac{\nu' - \lambda'}{r} \right) &= -\frac{\mathcal{G}^2}{2} + 8\pi p_t + \left[\frac{e^{-2\lambda}}{r^2} \left(2\mathcal{G} \right. \right. \\
& \times (e^\lambda - 3)\lambda'\nu' - 2(e^\lambda - 1)(2\mathcal{G}\nu'' \\
& + \mathcal{G}(\nu')^2) - 2r\nu'(2\mathcal{G}' - 3\mathcal{G}'\lambda') \\
& \left. \left. - 2\mathcal{G}'r(2\nu'' + (\nu')^2) \right) \right], \quad (9)
\end{aligned}$$

where (') manifests differentiation with respect to the radial coordinate. Solving these equations, we have

$$\begin{aligned}
\rho &= -\frac{1}{16\pi r^2} e^{-2\lambda} \left(\mathcal{G}^2 e^{2\lambda} r^2 - 4\mathcal{G}e^\lambda \lambda'\nu' + 12\mathcal{G}\lambda'\nu' + 8\mathcal{G}'e^\lambda \lambda' \right. \\
&- 24\mathcal{G}'\lambda' + 8\mathcal{G}e^\lambda \nu'' + 4\mathcal{G}e^\lambda (\nu')^2 - 16\mathcal{G}''e^\lambda - 8\mathcal{G}\nu'' - 4\mathcal{G}(\nu')^2 \\
&\left. + 16\mathcal{G}'' + 2e^\lambda - 2e^{2\lambda} - 2e^\lambda r\lambda' \right), \quad (10)
\end{aligned}$$

$$\begin{aligned}
p_r &= \frac{1}{16\pi r^2} e^{-2\lambda} \left(\mathcal{G}^2 e^{2\lambda} r^2 - 4\mathcal{G}e^\lambda \lambda'\nu' + 12\mathcal{G}\lambda'\nu' + 8\mathcal{G}e^\lambda \nu'' + 4\mathcal{G}e^\lambda (\nu')^2 \right. \\
&- 8\mathcal{G}'e^\lambda \nu' - 8\mathcal{G}\nu'' - 4\mathcal{G}(\nu')^2 + 24\mathcal{G}'\nu' + 2e^\lambda - 2e^{2\lambda} + 2e^\lambda r\nu' \left. \right), \quad (11)
\end{aligned}$$

$$\begin{aligned}
p_t &= \frac{1}{32\pi r^2} e^{-2\lambda} \left(2\mathcal{G}^2 e^{2\lambda} r^2 - 8\mathcal{G}e^\lambda \lambda'\nu' + 24\mathcal{G}\lambda'\nu' + 16\mathcal{G}e^\lambda \nu'' - 16\mathcal{G}\nu'' \right. \\
&+ 8\mathcal{G}e^\lambda (\nu')^2 - 8\mathcal{G}(\nu')^2 - 24\mathcal{G}'r\lambda'\nu' + 16\mathcal{G}'r\nu'' + 8\mathcal{G}'r(\nu')^2 + 16\mathcal{G}''r\nu' \\
&\left. - e^\lambda r^2 \lambda'\nu' + 2e^\lambda r^2 \nu'' + e^\lambda r^2 (\nu')^2 - 2e^\lambda r\lambda' + 2e^\lambda r\nu' \right). \quad (12)
\end{aligned}$$

The mass of a spherical object is one of the salient features which determines the total energy within the sphere. The definition of energy content within a given piece of the fluid distribution is not unique due to ambiguity in the localization of energy [43]. This problem exists in modified theories as well. However, researchers have used the definitions proposed by Tolman [44] as well as Misner-Sharp [45] to describe the mass of the distribution in modified theories. Hence, in the present work, mass function is characterized through Misner-Sharp definition as

$$m(r) = \frac{r}{2} (1 + g^{\delta\sigma} r_{,\delta} r_{,\sigma}),$$

which gives

$$e^{-\lambda(r)} = 1 - \frac{2m}{r}. \quad (13)$$

An n -dimensional spherical line element always belongs to embedding class-2. However, it can be embedded in an $n + 1$ -dimensional space if a symmetric tensor $b_{\xi\eta}$ satisfies the Gauss-Codazi equations

$$\mathcal{R}_{\xi\eta\mu\nu} = 2eb_{\xi[\mu}b_{\nu]\eta} \quad \text{and} \quad b_{\xi[\eta;\mu]} - \Gamma_{\eta\mu}^{\lambda}b_{\xi\lambda} + \Gamma_{\xi[\eta}^{\lambda}b_{\mu]\lambda} = 0. \quad (14)$$

Here, $e = \pm 1$ and $b_{\xi\eta}$ are the coefficients of second differential form. Eiesland [46] evaluated a necessary and sufficient condition for embedding class-1 as

$$\mathcal{R}_{0101}\mathcal{R}_{2323} = \mathcal{R}_{0202}\mathcal{R}_{1313} - \mathcal{R}_{1202}\mathcal{R}_{1303}, \quad (15)$$

and hence

$$(\lambda' - \nu')\nu' e^{\lambda} + 2(1 - e^{\lambda})\nu'' + \nu'^2 = 0. \quad (16)$$

Since both the metric potentials are unknown, so we assume one of them such that [12]

$$\nu(r) = 2\alpha r^2 + \ln \gamma, \quad (17)$$

where α and γ are positive constants. The existence of geometric as well as physical singularities inside the stellar models is a significant aspect in the analysis of compact structures. For this purpose, we investigate the behavior of metric function at the center of star. It is well-known that for physical validity of the solution, the metric potential must be positive, regular and monotonically increasing function within the entire stellar model [47]. We note that

$$\nu'(r) = 4\alpha r \quad \text{and} \quad \nu''(r) = 4\alpha.$$

It follows that $\nu(0) = \gamma$, $\nu'(0) = 0$ and $\nu''(0) > 0$ at the center. Hence, the chosen metric potential is free from singularity and monotonically increasing function having minimum at the center of the star. We use embedding class-1 approach to obtain $\lambda(r)$ from Eq.(18) as

$$\lambda(r) = \ln(1 + \beta\nu'^2 e^{\nu}), \quad (18)$$

where β is the integration constant. The behavior of metric functions at the center of compact objects is presented in Figure 1 which shows that the metric potentials satisfy the required physical conditions. We note that both the metric functions are minimum at the center and attain large values at the boundary of stars.

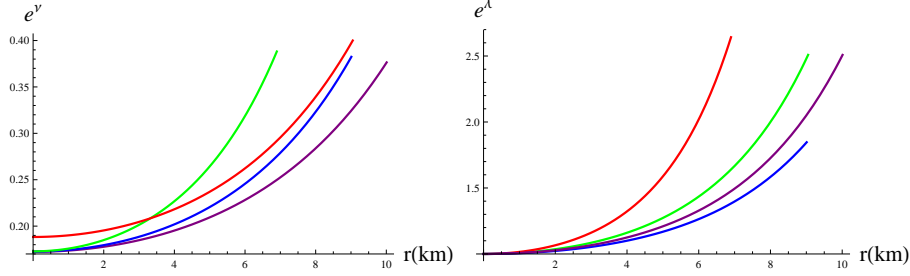


Figure 1: Plots of metric functions for Vela X-1 (green), SAX J1808.4-3658 (red), 4U 1608-52 (blue) and PSR J0348+0432 (purple) versus radial coordinate.

3 Matching with Exterior Metric

The set of constants (α, β, γ) interprets physical features as well as geometry of anisotropic stellar objects that can be evaluated by the smooth matching of interior (\mathcal{M}^-) and exterior (\mathcal{M}^+) spacetimes on the boundary (Σ) of the star. In general relativity, Jebsen-Birkhoff's theorem states that the gravitational field outside a spherically symmetric object is static. To define the exterior region of the compact stars, Schwarzschild solution is considered as the most appropriate choice. However, an exterior vacuum solution has not been evaluated in the context of $f(\mathcal{G})$ theory so many researchers [31, 32, 34] have used Schwarzschild metric to describe the exterior region of compact stars. Therefore in the present work, the external region is defined by the Schwarzschild metric as

$$ds^2 = \left(1 - \frac{2M}{r}\right) dt^2 - \left(1 - \frac{2M}{r}\right)^{-1} dr^2 - r^2(d\theta^2 + \sin^2\theta d\phi^2), \quad (19)$$

where M is the total mass. The continuity of metric coefficients at the boundary gives

$$e^{\nu(R)} = \gamma e^{2\alpha R^2} = 1 - \frac{2M}{R}, \quad e^{\lambda(R)} = 1 + 16\alpha^2\beta\gamma R^2 e^{2\alpha R^2} = \left(1 - \frac{2M}{R}\right)^{-1}. \quad (20)$$

Using Eqs.(17) and (20), we obtain

$$\alpha = \frac{M}{2R^2(R-2M)}, \quad \beta = \frac{R^3}{2M}, \quad \gamma = \frac{(R-2M)}{R} e^{\frac{M}{(2M-R)}}. \quad (21)$$

Substituting Eqs.(17) and (18) into (10)-(12), the energy density, radial and tangential pressures are

$$\begin{aligned}\rho &= \frac{1}{16\pi r(16\alpha^2\beta\gamma r^2 e^{2\alpha r^2} + 1)^3} \left[r(-1536\alpha^3\beta\mathcal{G}\gamma e^{2\alpha r^2}(2\alpha r^2 + 1) - \mathcal{G}^2 \right. \\ &\times (16\alpha^2\beta\gamma r^2 e^{2\alpha r^2} + 1)^3 + 256\alpha^2\beta\mathcal{G}''\gamma e^{2\alpha r^2}(16\alpha^2\beta\gamma r^2 e^{2\alpha r^2} + 1) \\ &+ 32\alpha^2\beta\gamma e^{2\alpha r^2}(256\alpha^4\beta^2\gamma^2 r^4 e^{4\alpha r^2} + 64\alpha^3\beta\gamma r^4 e^{2\alpha r^2} + 64\alpha^2\beta\gamma r^2 e^{2\alpha r^2} \\ &\left. + 4\alpha r^2 + 3)) - 512\alpha^2\beta\mathcal{G}'\gamma e^{2\alpha r^2}(2\alpha r^2 + 1)(8\alpha^2\beta\gamma r^2 e^{2\alpha r^2} - 1) \right], \quad (22)\end{aligned}$$

$$\begin{aligned}p_r &= \frac{1}{16\pi r(16\alpha^2\beta\gamma r^2 e^{2\alpha r^2} + 1)^3} \left[r(4096\alpha^6\beta^3\gamma^3 r^4 e^{6\alpha r^2}(\mathcal{G}^2 r^2 - 2) \right. \\ &+ 2048\alpha^5\beta^2\gamma^2 r^4 e^{4\alpha r^2} + 256\alpha^4\beta\gamma r^2 e^{2\alpha r^2}(3\beta\mathcal{G}^2\gamma r^2 e^{2\alpha r^2} - 4\beta\gamma e^{2\alpha r^2} \\ &+ 12\mathcal{G}) + 256\alpha^3\beta\gamma e^{2\alpha r^2}(6\mathcal{G} + r^2) + 16\alpha^2\beta\gamma e^{2\alpha r^2}(3\mathcal{G}^2 r^2 - 2) + 8\alpha \\ &\left. + \mathcal{G}^2) - 64\alpha\mathcal{G}'(128\alpha^4\beta^2\gamma^2 r^4 e^{4\alpha r^2} - 8\alpha^2\beta\gamma r^2 e^{2\alpha r^2} - 1) \right], \quad (23)\end{aligned}$$

$$\begin{aligned}p_t &= \frac{1}{16\pi r(16\alpha^2\beta r^2 e^{2\alpha r^2} + 1)^3} \left[r(4096\alpha^6\beta^3\mathcal{G}^2\gamma^3 r^6 e^{6\alpha r^2} + 128\alpha^4\beta\gamma r^2 \right. \\ &\times e^{2\alpha r^2}(6\beta\mathcal{G}^2 r^2 e^{2\alpha r^2} - 4\beta\gamma e^{2\alpha r^2} + 24\mathcal{G} + r^2) + 128\alpha^3\beta e^{2\alpha r^2}(12\mathcal{G} \\ &+ r^2) + 8\alpha^2(2\beta\gamma e^{2\alpha r^2}(3\mathcal{G}^2 r^2 - 2) + r^2) + 32\alpha\mathcal{G}''(16\alpha^2\beta r^2 e^{2\alpha r^2} \\ &\left. + 1) + 8\alpha + \mathcal{G}^2) - 32\alpha\mathcal{G}'(2\alpha r^2 + 1)(32\alpha^2\beta\gamma r^2 e^{2\alpha r^2} - 1) \right], \quad (24)\end{aligned}$$

where

$$\begin{aligned}\mathcal{G} &= -\frac{768\alpha^3\beta\gamma e^{2\alpha r^2}(1 + 2\alpha r^2)}{(1 + 16\alpha^2\beta\gamma e^{2\alpha r^2} r^2)^3}, \\ \mathcal{G}' &= \frac{1}{(1 + 16\alpha^2\beta\gamma e^{2\alpha r^2} r^2)^4} \left[6144\alpha^4\beta\gamma e^{2\alpha r^2} r(-1 + 12\alpha\beta\gamma e^{2\alpha r^2} \right. \\ &\left. - \alpha r^2 + 32\alpha^2\beta\gamma e^{2\alpha r^2} r^2 + 32\alpha^3\beta\gamma e^{2\alpha r^2} r^4) \right], \\ \mathcal{G}'' &= \frac{-1}{(1 + 16\alpha^2\beta\gamma e^{2\alpha r^2} r^2)^5} \left[6144\alpha^4\beta\gamma e^{2\alpha r^2}(1 + 5632\alpha^5\beta^2\gamma^2 e^{4\alpha r^2} r^6 \right. \\ &+ 4096\alpha^6\beta^2\gamma^2 e^{4\alpha r^2} r^8 + 16\alpha^3\beta\gamma e^{2\alpha r^2} r^2(84\beta\gamma e^{2\alpha r^2} - 43r^2) + 64\alpha^4 \\ &\times \beta\gamma e^{2\alpha r^2} r^4(64\beta\gamma e^{2\alpha r^2} - 7r^2) + 4\alpha^2 r^2(-76\beta\gamma e^{2\alpha r^2} + r^2) + \alpha \\ &\left. \times (-12\beta\gamma e^{2\alpha r^2} + 7r^2) \right].\end{aligned}$$

By using the Eqs.(21) and (23) with the condition $p_r(R) = 0$, we obtain the total mass of the compact stars as

$$M = \frac{1}{22} \left[13R - \frac{7R^2 \sqrt[3]{3}}{(-559R^3 + 44\sqrt{163}R^3)^{\frac{1}{3}}} + \frac{(-559R^3 + 44\sqrt{163}R^3)^{\frac{1}{3}}}{\sqrt[3]{3}} \right],$$

In anisotropic system, matter variables, i.e., matter density and pressure components are often related through EoS given as

$$\omega_r = \frac{p_r}{\rho}, \quad \omega_t = \frac{p_t}{\rho},$$

where ω_r and ω_t represent the EoS parameters. The presence of radial and tangential pressures in the stellar object yields the anisotropy which can be calculated from Eqs.(23) and (24) as

$$\begin{aligned} \Delta &= p_t - p_r = \frac{1}{2\pi r(16\alpha^2\beta\gamma r^2 e^{2\alpha r^2} + 1)^3} \left[\alpha(r(16\alpha^2\beta\gamma r^2 e^{2\alpha r^2} + 1)(\alpha r^2 \right. \\ &\times (1 - 8\alpha\beta\gamma e^{2\alpha r^2})^2 + 4\mathcal{G}'') + 4\mathcal{G}'(256\alpha^4\beta^2\gamma^2 r^4 e^{4\alpha r^2} - 64\alpha^3 \\ &\times \beta\gamma r^4 e^{2\alpha r^2} - 48\alpha^2\beta\gamma r^2 e^{2\alpha r^2} + 2\alpha r^2 - 1)) \Big]. \end{aligned} \quad (25)$$

4 Physical Analysis

In this section, we analyze various structural characteristics of the resulting anisotropic solutions, i.e., matter density, pressure components, anisotropic factor, energy constraints, mass function, compactness parameter, surface redshift and adiabatic index. For this purpose, we consider observed values of mass and predicted the radii from condition $p_r = 0$ at $r = R$ for star models, i.e., SAX J1808.4-3658, Vela X-1, PSR J0348+0432, and 4U 1608-52 [48]- [51]. The values of mass, predicted radii and matter values are presented in Table 1. Using these values, the unknown constants (α, β, γ) are calculated in Table 2. Moreover, the field equations (2) reduce to the Einstein field equations for $f(\mathcal{G}) = 0$. By following the technique in [12], we predict the radii and values of constants for the considered star models which are mentioned in Table 3. In $f(\mathcal{G})$ theory, the variation of matter variables and EoS parameter are shown in Figures 2 and 5, respectively whereas, Figures 3 and 6 exhibit the same attributes for the GR model. The plot of total mass is presented in Figure 4 which indicates that the anisotropic stellar structures

Table 1: Approximate values of physical parameters corresponding to $f(\mathcal{G}) = \mathcal{G}^2$ model for different stellar candidates.

Star Models	Mass (M_\odot)	Radius (km)	$\rho_c(gm/cm^3)$	$p_{rc}(dyne/cm^2)$
Vela X-1	1.77	9.05	1.3×10^{15}	3.6×10^{35}
SAX J1808.4-3658	1.43	6.9	2.4×10^{15}	8.4×10^{35}
4U 1608-52	1.74	9.01	1.4×10^{15}	9.7×10^{35}
PSR J0348+0432	2.1	10.06	1.2×10^{15}	4.2×10^{35}

Table 2: Approximate values of constants corresponding to $f(\mathcal{G}) = \mathcal{G}^2$ model for different stellar candidates.

Star Models	$\frac{m}{r}$	Z	α	β	γ
Vela X-1	0.29	1.4	0.0046	136.61	0.1883
SAX J1808.4-3658	0.31	1.5	0.0085	76.9	0.1728
4U 1608-52	0.30	1.6	0.0049	131.8	0.1726
PSR J0348+0432	0.29	1.51	0.0039	131.8	0.1723

become more massive as the radius increases. The graphical behavior shows that energy density as well as pressure components exhibit large values as compared to GR [53]. Moreover, the EoS parameters lie within the interval (0,1) and attain higher values as compared to GR [15]. The positive and regular behavior of these variables ensure the singularity-free nature of the matter components. It is observed that anisotropic system is more dense in modified Gauss-Bonnet gravity in comparison to GR [53].

The pressure anisotropy helps us to analyze the matter distribution and its direction depends on radial and transversal pressures. If $p_t > p_r$, then anisotropy is positive which shows the outward directed pressure whereas the case $p_t < p_r$ gives negative anisotropy which indicates inward directed pressure. Figure 2 shows repulsive nature of anisotropic force which is required for stellar structures [52]. Moreover, the graphical analysis also exhibits that anisotropy increases in the framework of $f(\mathcal{G})$ gravity as compared to GR [15].

Table 3: Approximate values of physical parameters and constants when $f(\mathcal{G}) = 0$.

Star Models	Mass (M_{\odot})	Radius (km)	α	$16\alpha\beta\gamma$
Vela X-1	1.77	8.93	0.0032	2.40
SAX J1808.4-3658	1.43	6.75	0.0054	2.45
4U 1608-52	1.74	8.80	0.0026	2.65
PSR J0348+0432	2.10	9.70	0.0031	2.20

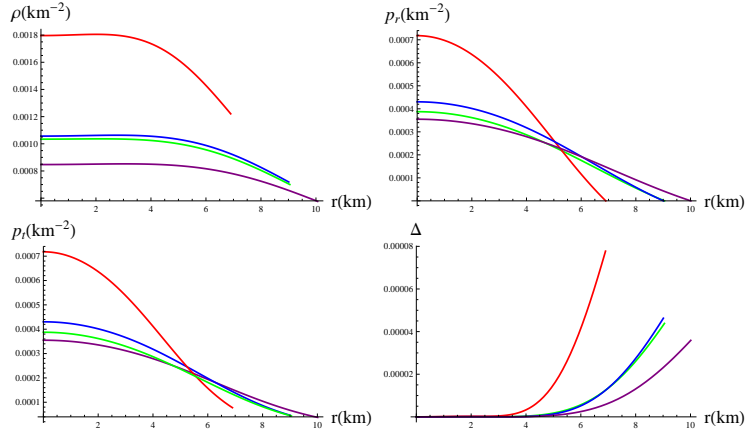


Figure 2: Variation of matter density, radial pressure, transversal pressure and anisotropy for $f(\mathcal{G}) = \mathcal{G}^2$ model corresponding to SAX J1808.4-3658 (red), Vela X-1 (green), 4U 1608-52 (blue) and PSR J0348+0432 (purple) against radial coordinate.

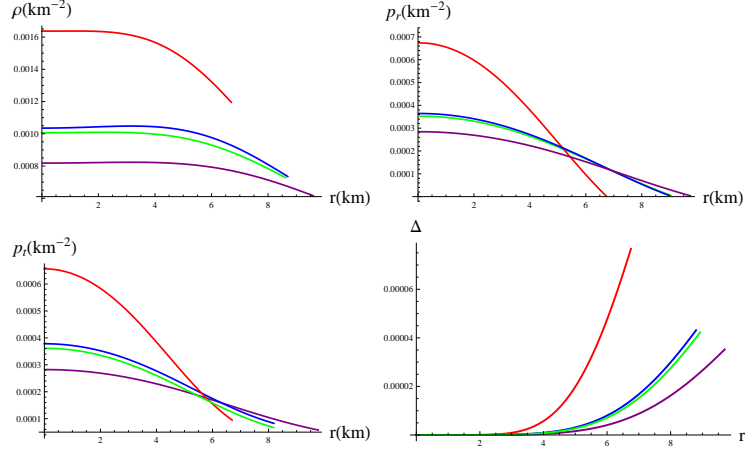


Figure 3: Variation of matter density, radial pressure, transversal pressure and anisotropy for SAX J1808.4-3658 (red), Vela X-1 (green), 4U 1608-52 (blue) and PSR J0348+0432 (purple) against radial coordinate for $f(\mathcal{G}) = 0$.

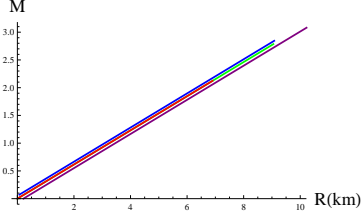


Figure 4: Analysis of total mass verses radius corresponding to SAX J1808.4-3658 (red), Vela X-1 (green), 4U 1608-52 (blue) and EXO 1785-248 (purple).

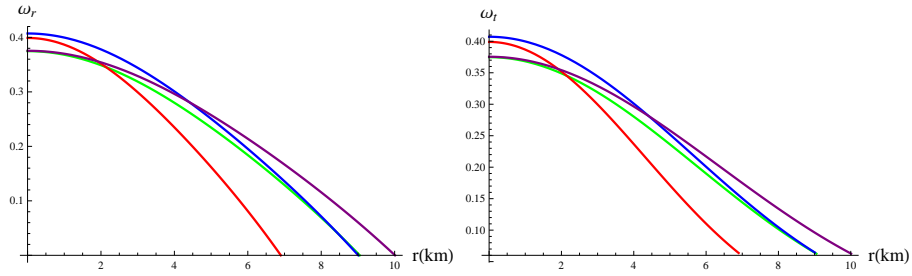


Figure 5: Variation of EoS parameters for $f(\mathcal{G}) = \mathcal{G}^2$ model corresponding to SAX J1808.4-3658 (red), Vela X-1 (green), 4U 1608-52 (blue) and PSR J0348+0432 (purple) against radial coordinate.

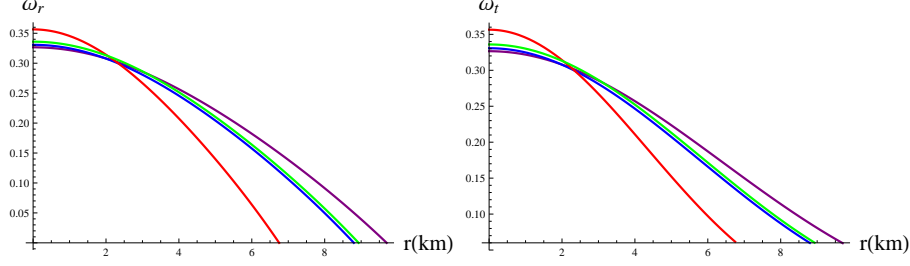


Figure 6: Variation of EoS parameters for SAX J1808.4-3658 (red), Vela X-1 (green), 4U 1608-52 (blue) and PSR J0348+0432 (purple) against radial coordinate when $f(\mathcal{G}) = 0$.

4.1 Energy Bounds

The presence of ordinary or exotic matter inside the stellar geometry is ensured by energy bounds. These conditions are classified into null, weak, dominant and strong which must be satisfied for the realistic existence of ordinary matter. For anisotropic matter source, these conditions are

- Null: $\rho + p_r \geq 0, \quad \rho + p_t \geq 0,$
- Weak: $\rho \geq 0, \quad \rho + p_r \geq 0, \quad \rho + p_t \geq 0,$
- Dominant: $\rho - p_r \geq 0, \quad \rho - p_t \geq 0,$
- Strong: $\rho + 2p_t + p_r \geq 0.$

Figure 7 depicts that all the energy bounds are fulfilled which confirm the presence of ordinary matter in compact star models. Moreover, we also check the energy conditions when $f(\mathcal{G}) = 0$. The graphical behavior (Figure 8) confirms the presence of normal matter inside the star models. The validity of energy conditions also leads to the physical viability of the solution. It is worthwhile to mention here that for larger negative values of χ energy conditions are violated in the present work.

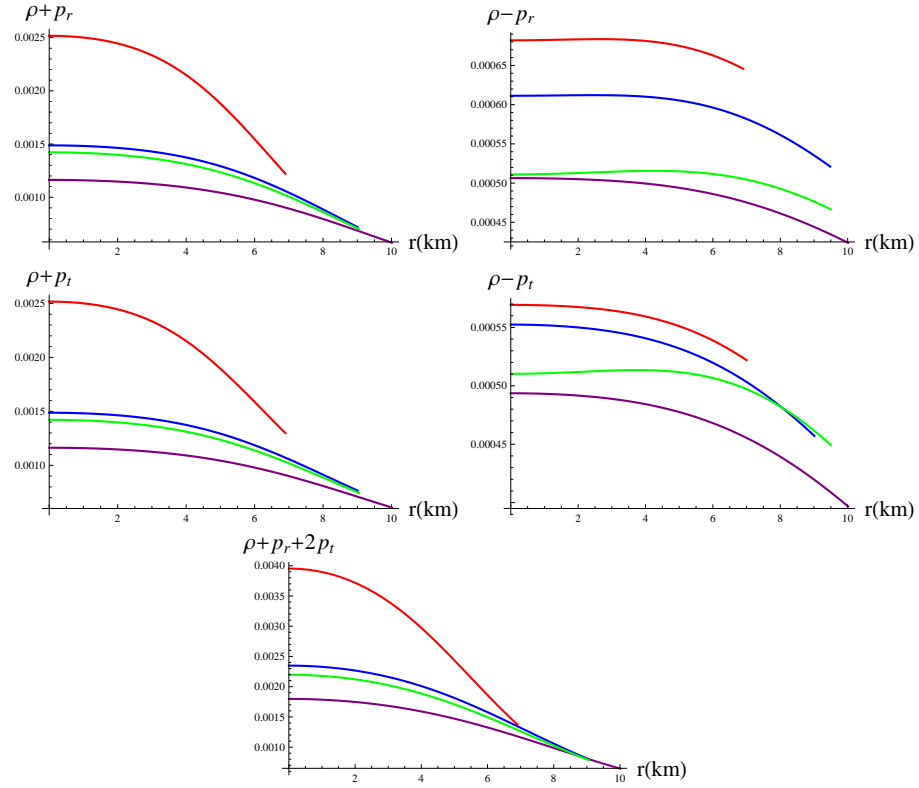


Figure 7: Energy bounds for $f(\mathcal{G}) = \mathcal{G}^2$ model corresponding to SAX J1808.4-3658 (red), Vela X-1 (green), 4U 1608-52 (blue) and EXO 1785-248 (purple).

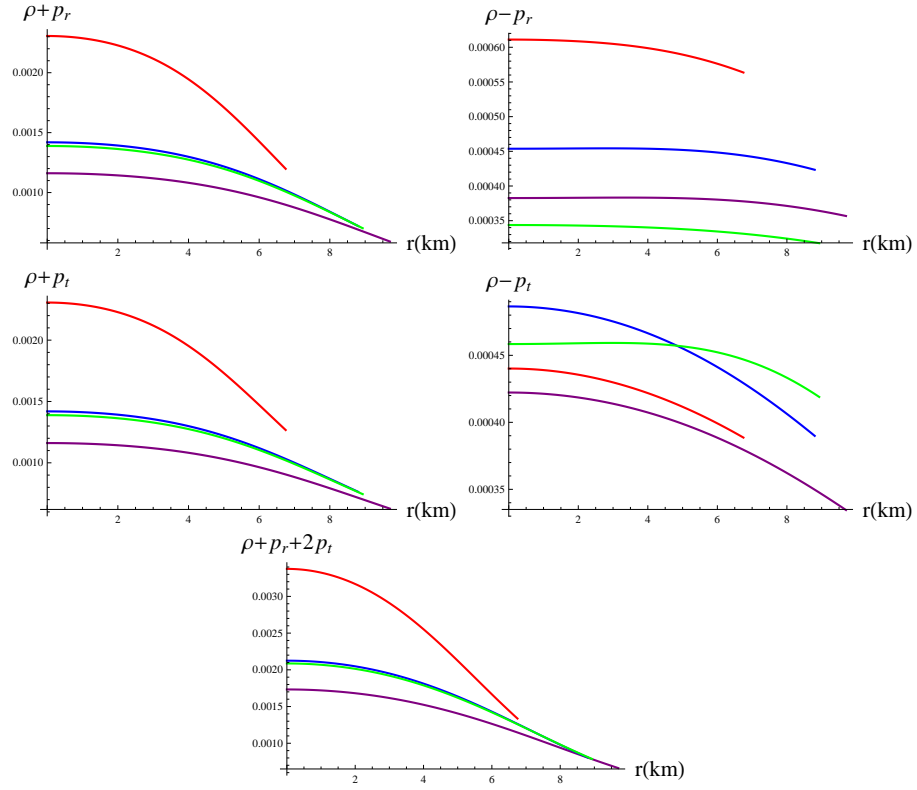


Figure 8: Energy bounds for SAX J1808.4-3658 (red), Vela X-1 (green), 4U 1608-52 (blue) and EXO 1785-248 (purple) when $f(\mathcal{G}) = 0$.

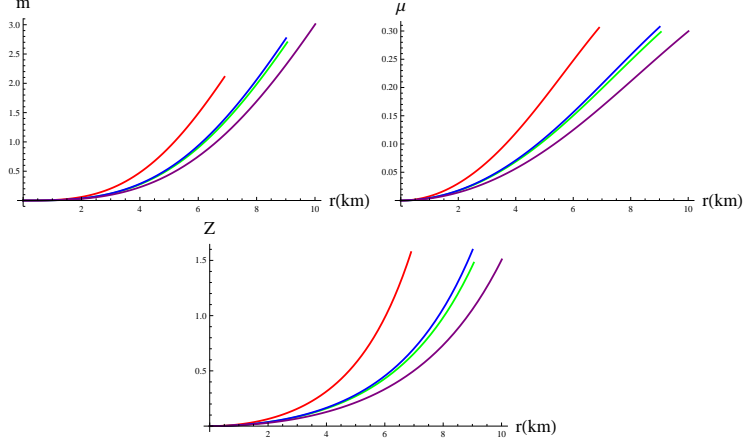


Figure 9: Analysis of mass, compactness parameter and gravitational redshift for $f(\mathcal{G}) = \mathcal{G}^2$ model corresponding to SAX J1808.4-3658 (red), Vela X-1 (green), 4U 1608-52 (blue) and EXO 1785-248 (purple).

4.2 Mass, Compactness and Redshift

The mass of anisotropic stellar object through Eq.(15) turns out to be

$$m = \frac{Mr^3 e^{\frac{M(R^2-r^2)}{R^2(2M-R)}}}{R^2(R-2M) + 2Mr^2 e^{\frac{M(R^2-r^2)}{R^2(2M-R)}}}, \quad (26)$$

which shows that mass and radius are inter-related quantities such that the mass becomes zero at $r = 0$. The regular behavior for mass of the stars is verified through graphical analysis in Figure 5. We also observe that mass of stellar objects increases as the radius increases. The compactness function is defined as the mass to radius ratio for the celestial bodies given by

$$\mu(r) = \frac{m(r)}{r} = \frac{Mr^2 e^{\frac{M(R^2-r^2)}{R^2(2M-R)}}}{R^2(R-2M) + 2Mr^2 e^{\frac{M(R^2-r^2)}{R^2(2M-R)}}}. \quad (27)$$

The gravitational redshift is considered as an important element to examine the physical behavior of celestial bodies as it measures the force exerted on light due to strong gravity. It is defined as $Z = -1 + \frac{1}{\sqrt{1-2\mu(r)}}$, which

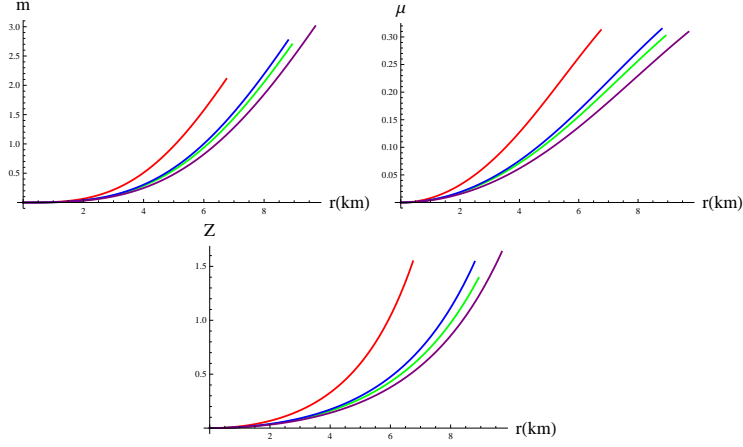


Figure 10: Analysis of mass, compactness parameter and gravitational redshift for SAX J1808.4-3658 (red), Vela X-1 (green), 4U 1608-52 (blue) and EXO 1785-248 (purple) when $f(\mathcal{G}) = 0$.

yields

$$Z = -1 + \sqrt{1 + \frac{2Mr^2 e^{\frac{M(R^2-r^2)}{R^2(2M-R)}}}{R^2(R-2M)}}. \quad (28)$$

Figure 9 demonstrates the monotonic increasing nature of compactness factor corresponding to different stellar models which satisfies the Buchdahl condition ($\frac{m}{r} < \frac{4}{9}$) [54]. The gravitational redshift is also found to be monotonically increasing function of radial coordinate and satisfies the range for anisotropic compact stars, $Z \leq 5.211$ [55]. Figure 10 exhibits that these parameters are consistent with their respective limits for the GR model.

4.3 Stability of Compact Stars

Here, we discuss TOV equation, causality condition and adiabatic index in the context of $f(\mathcal{G})$ gravity. This will help us to examine the equilibrium and stable behavior of the obtained solution. Astashenok et al. [56]-[59] studied the internal structure of neutron star for different models and also discussed the modified TOV equation in $f(\mathcal{R})$ and $f(\mathcal{G})$ theories of gravity. The corresponding TOV equation is constructed from the continuity equation

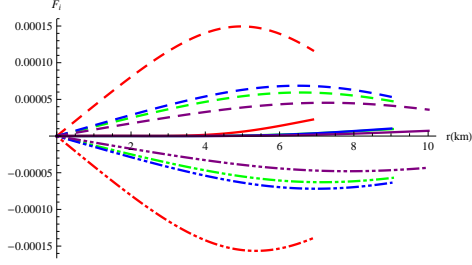


Figure 11: Behavior of different forces F_h (dashed lines), F_a (solid lines) and F_g (dotted dashed lines) for $f(\mathcal{G}) = \mathcal{G}^2$ model corresponding to SAX J1808.4-3658 (red), Vela X-1 (green), 4U 1608-52 (blue) and PSR J0348+0432 (purple).

($\nabla^\alpha T_{\alpha\beta} = 0$) as

$$\frac{-\nu'}{2}(\rho + p_r) - \frac{dp_r}{dr} + \frac{2}{r}(p_t - p_r) = 0, \quad (29)$$

where $\frac{-\nu'}{2}(\rho + p_r)$ depicts the gravitational force (F_g), $-\frac{dp_r}{dr}$ represents the hydrodynamic force (F_h) and $\frac{2}{r}(p_t - p_r)$ indicates the anisotropic force F_a . Figure 11 indicates that the sum of all these forces is zero, i.e., $F_g + F_a + F_h = 0$ which assures the existence of the equilibrium system.

A stable stellar system is considered to be more realistic from astrophysical point of view. It is necessary to inspect the behavior of the matter source after its departure from the state of equilibrium, when non-vanishing radial forces of different signs appear within the system. We examine stability of the solution through causality condition and adiabatic index. To preserve the causality condition, the stable anisotropic spherical objects must have speed of sound less than that of light [60], i.e., $0 < v_r^2 < 1$ and $0 < v_t^2 < 1$, where v_r and v_t represent the radial and tangential components of sound speeds, respectively expressed as

$$v_r^2 = \frac{dp_r}{d\rho}, \quad v_t^2 = \frac{dp_t}{d\rho}. \quad (30)$$

To examine the potentially stable or unstable structures of stellar objects, we consider Herrera's cracking approach [61]. Accordingly, celestial objects should satisfy the inequality $0 < |v_t^2 - v_r^2| < 1$ for potentially stable model. Figures 12 and 13 indicate that square of the radial and tangential sound

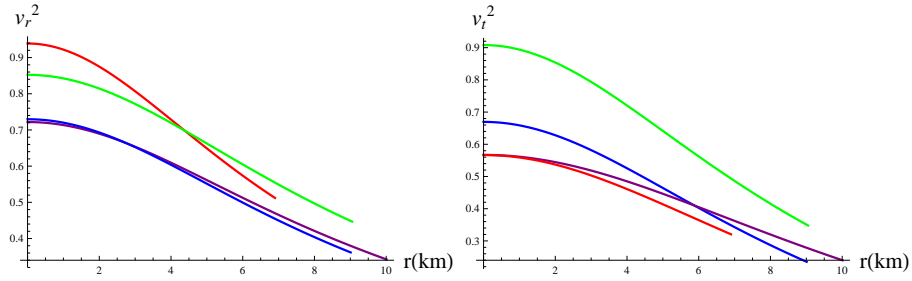


Figure 12: Variation of radial and tangential sound speeds for $f(\mathcal{G}) = \mathcal{G}^2$ model corresponding to SAX J1808.4-3658 (red), Vela X-1 (green), 4U 1608-52 (blue) and PSR J0348+0432 (purple).

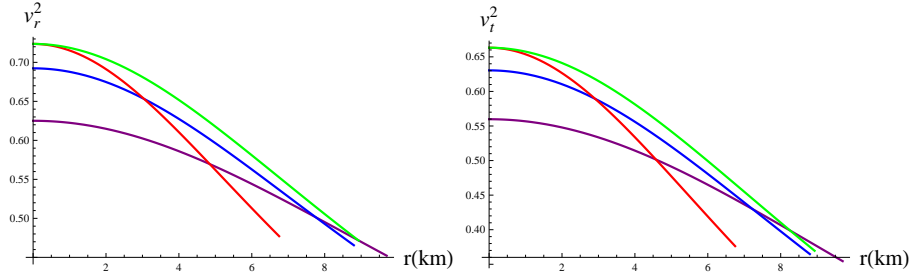


Figure 13: Variation of radial and tangential sound speeds for SAX J1808.4-3658 (red), Vela X-1 (green), 4U 1608-52 (blue) and PSR J0348+0432 (purple) when $f(\mathcal{G}) = 0$.

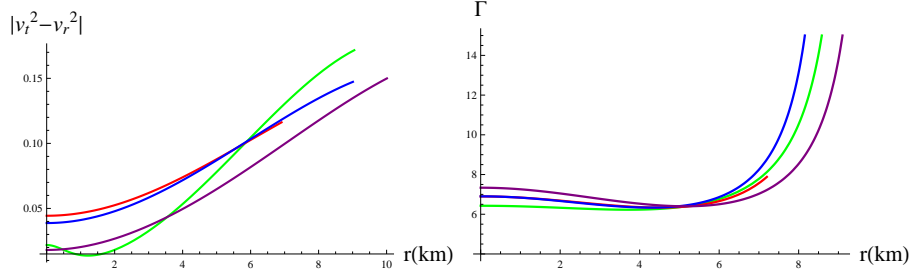


Figure 14: Behavior of $0 < |v_t^2 - v_r^2| < 1$ and adiabatic index for $f(\mathcal{G}) = \mathcal{G}^2$ model corresponding to SAX J1808.4-3658 (red), Vela X-1 (green), 4U 1608-52 (blue) and PSR J0348+0432 (purple).

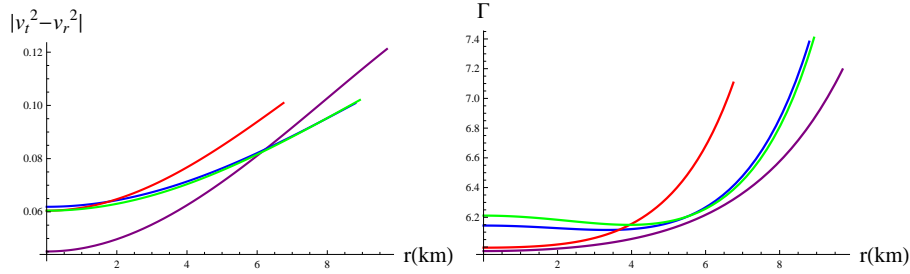


Figure 15: Behavior of $0 < |v_t^2 - v_r^2| < 1$ and adiabatic index for SAX J1808.4-3658 (red), Vela X-1 (green), 4U 1608-52 (blue) and PSR J0348+0432 (purple) when $f(\mathcal{G}) = 0$.

speeds satisfy the causality condition in $f(\mathcal{G})$ theory and GR, respectively. Moreover, the plots of absolute value of the difference of radial and tangential velocities (Figures 14 and 15 - left panels) lie in the prescribed bounds of Herrera's cracking approach.

For a given energy density, the adiabatic index (Γ) illustrates the stability of relativistic as well as non-relativistic celestial objects. The adiabatic index is a stiffness parameter which measures the change in pressure corresponding to a small change in density. According to Heintzmann and Hillebrandt [62], the adiabatic index must be greater than $\frac{4}{3}$ for the stable stellar models. The adiabatic index in mathematical form is defined as

$$\Gamma = \frac{p_r + \rho}{p_r} \frac{dp_r}{d\rho} = \frac{p_r + \rho}{p_r} v_r^2. \quad (31)$$

Figures 14 and 15 (right panels) exhibit that the value of adiabatic index

is in the defined range, i.e., greater than $\frac{4}{3}$, for all star models. Thus, the resulting solution shows dynamically stable behavior in $f(\mathcal{G})$ theory as well as in GR [12].

5 Concluding Remarks

The purpose of this paper is to analyze the embedding class-1 solution for anisotropic spherically symmetric compact stars in $f(\mathcal{G})$ gravity. We have smoothly matched the interior spacetime with the exterior Schwarzschild metric to find the arbitrary constants (α, β, γ) . The observed masses of SAX J1808.4-3658, Vela X-1, PSR J0348+0432 and 4U 1608-52 have been employed to predict the radii through the condition $p_r(R) = 0$. The results are summarized as follows.

- We have observed that both metric functions have the lowest values at the core of stellar models and then monotonically increase towards the boundary. We have found that our metric functions are compatible and fulfill all the required constraints.
- The energy density, tangential/radial pressure depict maximum values at the core and minimum values at the surface of the stars which confirms the viable physical structures of compact objects. The behavior of anisotropy is obtained such that it is zero at the center and becomes maximum at the boundary of the system. Moreover, EoS parameters lie in the accepted range, i.e., $0 < \omega_r < 1$ and $0 < \omega_t < 1$.
- The energy conditions are satisfied assuring the presence of normal distribution of matter inside the compact stellar structures.
- The compactness and redshift parameters satisfy the required range, i.e., $\frac{m}{r} < \frac{4}{9}$ and $Z < 5.211$, respectively.
- The physical behavior of three forces, F_g , F_h and F_a confirms the state of equilibrium for anisotropic spherical solution.
- Finally, we have checked stability of the system through causality, Herrera conditions and adiabatic index. These conditions are satisfied demonstrating that our anisotropic compact model is stable.

We conclude that the embedding class-1 technique in $f(\mathcal{G})$ framework is compatible as all the structural attributes of stellar models follow the physically accepted criteria. It is worth mentioning here that anisotropic interior solutions in this theory represent more dense structures as compared to GR [12, 15, 53].

References

- [1] Ruderman, A.: Annu. Rev. Astron. Astrophys. **10**(1972)427.
- [2] Sawyer, R.F.: Phys. Rev. Lett. **29**(1972)382.
- [3] Sokolov, A.I.: J. Exp. Theor. Phys. **79**(1980)1137.
- [4] Kippenhahn, R.K. and Weigert, A.: Stellar Structure and Evolution (Springer, 1990).
- [5] Herrera, L. and Santos, N.O.: Phys. Rep. **286**(1997)53.
- [6] Harko, T. and Mak, M.K.: Annalen Phys. **11**(2002)3.
- [7] Dev, K. and Gleiser, M.: Gen. Relativ. Gravit. **39**(2002)1793; *ibid.* **35**(2003)1435.
- [8] Hossein, S.K.M. et al.: Int. J. Mod. Phys. D **21**(2012)1250088.
- [9] Paul, B.C. and Deb, R.: Astrophys. Space Sci. **354**(2014)421.
- [10] Eisenhart, L.P.: *Riemannian Geometry* (Princeton University Press, 1925).
- [11] Maurya, S.K. et al.: Eur. Phys. J. A **52**(2016)191.
- [12] Maurya, S.K. et al.: Eur. Phys. J. C **76**(2016)266.
- [13] Singh, K.N. and Pant, N.: Eur. Phys. J. C **76**(2016)524.
- [14] Bhar, P. et al.: Eur. Phys. J. A **52**(2016)312.
- [15] Singh, K.N. et al.: Eur. Phys. J. A **53**(2017)21.
- [16] Capozziello, S. et al.: Phys. Rev. D **83** (2011)064004.

- [17] Nojiri, S. and Odintsov, S.D.: Phys. Rep. **505**(2011)59.
- [18] Olmo, G.J.: Int. J. Mod. Phys. D **20**(2011)413.
- [19] Zubair, M and Abbas, G.: Astrophys. Space Sci. **361**(2016)342.
- [20] Yousaf, Z. et al.: Eur. Phys. J. C **77**(2017)691.
- [21] Nojiri, S. and Odintsov, S.D.: Phys. Lett. B **631**(2005)1.
- [22] Nojiri, S. and Odintsov, S.D.: Int. J. Geom. Meth. Mod. Phys. **04**(2007)115.
- [23] Bamba, K. et al.: Eur. Phys. J. C **67**(2010)295.
- [24] Nojiri, S. and Odintsov, S.D.: Phys. Rept. **505**(2011)59.
- [25] Oikonomou, V.K.: Phys. Rev. D **92**(2015)124027.
- [26] Nojiri, S. et al.: Phys. Rept. **692**(2017)1.
- [27] Felice, A. and Tanaka, T.: Prog. Theor. Phys. **124**(2010)503.
- [28] Nojiri, S. et al.: Phys. Rev. D **99**(2019)044050.
- [29] Nojiri, S. et al.: Eur. Phys. J. C **79**(2019)565.
- [30] Akrami, Y. et al.: Astron. Astrophys. **641**(2020)A10.
- [31] Abbas, G. et al.: Astrophys. Space Sci. **357**(2015)158.
- [32] Sharif, M. and Fatima, I.: Int. J. Mod. Phys. D **25**(2016)1650083.
- [33] Sharif, M. and Naz, S.: Mod. Phys. Lett. A **33**(2018)1850109.
- [34] Sharif, M. and Saba, S.: Eur. Phys. J. C **78**(2018)921.
- [35] Sharif, M. and Saba, S.: Chin. J. Phys. **59**(2019)481.
- [36] Odintsov, S.D. et al.: arXiv:2003.13724.
- [37] Oikonomou, V.K. and Fronimos, F.P.: arXiv:2006.05512.
- [38] Astasheonk, A.V. et al.: arXiv:2008.10884.

- [39] Abbott, R. et al.: *Astrophys. J. Lett.* **896**(2020)2.
- [40] Shamir, M.F. and Naz, T.: *Phys. Dark Universe.* **27**(2020)100472.
- [41] Cognola, G. et al.: *Phys. Rev. D* **73**(2006)084007.
- [42] Shamir, M.F.: *Astrophys. Space Sci.* **362**(2017)67.
- [43] Herrera, L. and Santos, N.O.: *Phys. Reports* **286**(1997)53.
- [44] Tolman, R.C.: *Phys. Rev.* **35**(1930)875.
- [45] Misner, C.W. and Sharp, D.H.: *Phys. Rev.* **136**(1964)B571.
- [46] Eiesland, J.: *Trans. Am. Math. Soc.* **27**(1925)213.
- [47] Lake, K.: *Phys. Rev. D* **67**(2003)104015.
- [48] Güver, T. et al.: *Astrophys. J.* **712**(2010)96.
- [49] Rawls, M.L. et al: *Astrophys. J.* **730**(2011)25.
- [50] Maurya, S.K. et al.: *Eur. Phys. J. C* **75**(2015)389.
- [51] Maurya, S.K. et al.: *Eur. Phys. J. C* **76**(2016)693.
- [52] Gokhroo, M.K. and Mehra, A.L.: *Gen. Relativ. Gravit.* **26**(1994)75.
- [53] Deb, D. et al.: *Ann. Phys.* **387**(2017)239.
- [54] Buchdahl, A.H.: *Phys. Rev. D* **116**(1959)1027.
- [55] Ivanov, B.V.: *Phys. Rev. D* **65**(2002)104011.
- [56] Astashenok, A.V et al.: *J. Cosmol. Astropart. Phys.* **12**(2013)040.
- [57] Astashenok, A.V et al.: *Phys. Rev. D* **89**(2014)103509.
- [58] Astashenok, A.V et al.: *J. Astrophys. Space. Sci.* **355**(2014)333.
- [59] Astashenok, A.V et al.: *J. Cosmol. Astropart. Phys.* **01**(2015)001.
- [60] Abreu, H. et al.: *Class. Quantum Gravit.* **24**(2007)4631.
- [61] Herrera, L.: *Phys. Let. A* **165**(1992)206.
- [62] Heintzmann, H. and Hillebrandt, W.: *Astron. Astrophys.* **38**(1975)51.